Effects of frequency mismatch on amplitude death in delay-coupled oscillators

Effects of frequency mismatch on amplitude death in delay-coupled oscillators

Shinsuke Mizukami,[1] Keiji Konishi,[1,*] Yoshiki Sugitani,[2] Takahiro Kouda,[1] and Naoyuki Hara[1]
[1]*Department of Electrical and Information Systems, Osaka Prefecture University, 1-1 Gakuen-cho, Naka-ku, Sakai, Osaka 599-8531, Japan*
[2]*Department of Electrical and Electronic Systems Engineering, Ibaraki University, 4-12-1 Nakanarusawa, Hitachi, Ibaraki 316-8511, Japan*

(Received 26 July 2021; accepted 18 October 2021; published 15 November 2021)

The present paper analytically reveals the effects of frequency mismatch on the stability of an equilibrium point within a pair of Stuart-Landau oscillators coupled by a delay connection. By analyzing the roots of the characteristic function governing the stability, we find that there exist four types of boundary curves of stability in a coupling parameters space. These four types depend only on the frequency mismatch. The analytical results allow us to design coupling parameters and frequency mismatch such that the equilibrium point is locally stable. We show that, if we choose appropriate frequency mismatches and delay times, then it is possible to induce amplitude death with strong stability, even by weak coupling. In addition, we show that parts of these analytical results are valid for oscillator networks with complete bipartite topologies.

DOI: 10.1103/PhysRevE.104.054207

I. INTRODUCTION

A variety of phenomena occur in coupled oscillators [1,2]. Quenching, an attractive phenomenon, has received broad attention for over 30 years [3–6]. This phenomenon is roughly classified into two types: amplitude death, a coupling-induced stabilization of equilibrium points embedded within oscillators, and oscillation death, a coupling-induced emergence of stable equilibrium points in oscillators [7,8].

Amplitude death has been intensively studied not only from viewpoints of academia [7–9], but also from viewpoints of engineering [10,11], because of the ability of amplitude death to suppress undesired oscillations with noninvasive coupling signals. It has been reported that a simple diffusive connection never induces amplitude death in oscillators *without* frequency mismatch (i.e., in identical oscillators). However, *with* frequency mismatch, amplitude death can be induced [5,6]. Reddy, Sen, and Johnston discovered that a time-delayed connection, which is the natural diffusive connection with finite-speed propagation of information, can induce amplitude death in oscillators, even *without* frequency mismatch [12–14]. Such delay-coupled-induced amplitude death has been investigated in a large number of studies. Delay-induced amplitude death can be observed in oscillator networks [12,13,15–19]. In order to enlarge the parameter sets in which delay-induced amplitude death occurs, the time-delayed connection has been modified. Examples include distributed delay connection [20,21], partial delay connection [22], two delay connections [23], digital delay connection [24], and time-varying delay connection [25,26].

Considerable knowledge of delay-induced amplitude death has been accumulated, as mentioned above. In recent years, such knowledge has been widely applied in several fields, including chemical reaction systems [27], candle-flame systems [28–31], thermoacoustic systems [11,32–36], aeroelastic systems [37], fractional-order systems [38–40], and reaction-diffusion systems [41]. Very recently, in addition to such applications, studies have examined amplitude death with partial death [42,43], with analytical treatment for heterogeneous delays [44,45], with time-varying network topology [46], with asymmetric connection delays [47], with an additional mean-field feedback [48], and on stability islands [49].

Analytical studies on the stability of equilibrium points within delay-coupled oscillators play an important role in the further development of knowledge about delay-induced amplitude death. This is because such studies, which provide analytical deep insights about the corresponding properties, have the potential to be widely used in various fields and for a variety of applications. Most of these analytical studies, however, have concentrated on oscillators *without* frequency mismatch [15–19,49] because the characteristic function governing the stability without mismatch can be reduced to a simple function by some straightforward manipulations. In other words, frequency mismatch, one of the most important factors for coupled oscillators, makes the analytical treatment of the characteristic function difficult. As a result, to our knowledge, there has been a great lack of analytical comprehending effects of the frequency mismatch on delay-induced amplitude death.

The present paper deals with analytical studies on stability *with* frequency mismatch from the stability analysis [50–53] used in the control community. We reveal the effects of frequency mismatch on the stability of the equilibrium points within delay-coupled oscillators. The critical delays of stability with frequency mismatch are analytically derived. Furthermore, we provide a procedure for designing delayed connections inducing amplitude death. Note that pioneering research in this field [12,13] analytically derived the critical delays without frequency mismatch. However, critical delays with mismatch were obtained by numerically solving the characteristic function.

*URL: http://www2.eis.osakafu-u.ac.jp/∼ecs

The remainder of the present paper is organized as follows. Section II reviews a pair of Stuart-Landau oscillators with frequency mismatch and yields the characteristic function at the equilibrium point. Section III elucidates the roots of the characteristic function located on the imaginary axis and analytically derives the critical delays. Section IV designs the coupling parameters and the mismatch such that the equilibrium point within the coupled oscillators is stable. Section V extends the obtained results to oscillator networks with complete bipartite topologies and presents numerical examples.

II. DELAY-COUPLED STUART-LANDAU OSCILLATORS

We consider a pair of Stuart-Landau oscillators:

$$\dot{Z}_{1,2}(t) = \{1 + i\Omega_{1,2} - |Z_{1,2}(t)|^2\}Z_{1,2}(t) + K\{Z_{2,1}(t-\tau) - Z_{1,2}(t)\}, \tag{1}$$

where $Z_{1,2}(t) \in \mathbb{C}$ are respectively the states of oscillators 1 and 2 at time $t \geqslant 0$. The imaginary unit is denoted as $i := \sqrt{-1}$. The oscillators have frequencies of $\Omega_{1,2} > 0$, a coupling strength of $K \geqslant 0$, and a delay time of $\tau \geqslant 0$. The frequencies are given as

$$\Omega_1 := \overline{\Omega} + \frac{\Delta}{2}, \quad \Omega_2 := \overline{\Omega} - \frac{\Delta}{2},$$

where $\overline{\Omega} > 0$ is the nominal frequency, and $\Delta \in [0, 2\overline{\Omega})$ represents the frequency mismatch.

The delay-coupled oscillators (1) have the equilibrium point $Z_1^* = Z_2^* = 0$. The linearized dynamics of oscillators (1) at the equilibrium point is described by

$$\dot{z}_{1,2}(t) = (1 - K + i\Omega_{1,2})z_{1,2}(t) + Kz_{2,1}(t-\tau), \tag{2}$$

where $z_{1,2}(t) := Z_{1,2}(t) - Z_{1,2}^*$ are small perturbations around the equilibrium point. The stability of linear system (2), which is equivalent to the local stability of the equilibrium point, is governed by the characteristic function [12,13]:

$$g(s,\tau) := (s - 1 + K - i\Omega_1)(s - 1 + K - i\Omega_2) - K^2 e^{-2s\tau}. \tag{3}$$

As shown in Fig. 1, the characteristic roots $s \in \mathbb{C}$ of $g(s,\ \tau)$ move as a function of the delay time τ in the complex plane. The stability changes when a root crosses the imaginary axis. Now, we focus on the behavior of the roots located on the axis. By substituting $s = i\omega$, $\omega \in \mathbb{R}^+$ into $g(s,\ \tau) = 0$,[1] we have its real and imaginary parts [12,13]:

$$(\omega - \overline{\Omega})^2 - \frac{\Delta^2}{4} - (1-K)^2 + K^2\cos 2\omega\tau = 0, \tag{4a}$$

$$2(1-K)(\omega - \overline{\Omega}) - K^2 \sin 2\omega\tau = 0. \tag{4b}$$

Here, ω satisfying both Eqs. (4a) and (4b) are denoted by $\omega = \omega_{++,+-,--,-+}$,

$$\omega_{++} := \overline{\Omega} + \sqrt{p_+(\Delta,K)}, \quad \omega_{+-} := \overline{\Omega} + \sqrt{p_-(\Delta,K)},$$
$$\omega_{--} := \overline{\Omega} - \sqrt{p_-(\Delta,K)}, \quad \omega_{-+} := \overline{\Omega} - \sqrt{p_+(\Delta,K)}, \tag{5}$$

[1]Our analysis can be restricted to $\omega \in \mathbb{R}^+$ without loss of generality.

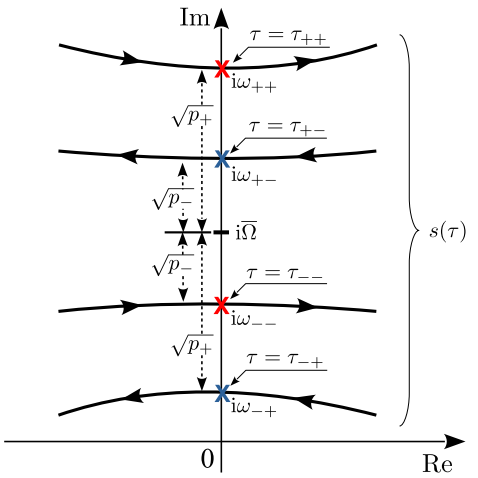

FIG. 1. Sketch of roots s around the imaginary axis on the complex plane (see Lemma 2): roots can cross the imaginary axis via stabilizing points $i\omega_{+-,-+}$ (blue crosses) and the destabilizing points $i\omega_{++,--}$ (red crosses) at $\tau = \tau_{+-,-+,++,--}$.

where $p_\pm(\Delta, K)$ are defined as

$$p_\pm(\Delta,K) := \Delta^2/4 - (1-K)^2 \pm \sqrt{q(\Delta,K)}, \tag{6}$$

$$q(\Delta,K) := K^4 - (1-K)^2\Delta^2. \tag{7}$$

The roots s moving with τ can cross the imaginary axis at, at most, the four points $i\omega_{++,+-,--,-+}$, as depicted in Fig. 1. Note that previous studies [12,13] dealt only with the two crossing points $i\omega_{++,-+}$ for the case of $\Delta = 0$.[2] This is because the other crossing points $i\omega_{+-,--}$ do not exist due to $p_-(\Delta,K) < 0$ for $\Delta = 0$. Thus, the frequency mismatch is necessary for existence of the four crossing points $i\omega_{++,+-,--,-+}$.

III. STABILITY ANALYSIS

This section reveals the relation of the crossing points $i\omega_{++,+-,--,-+}$ to the frequency mismatch Δ and the coupling strength K. The directions of the roots crossing these points and the delays at these points will be analytically provided.

A. Existence of crossing points $i\omega_{++,+-,--,-+}$

This subsection focuses on the regions in parameter space (Δ, K) where there exist crossing points $i\omega_{++,+-,--,-+}$. Equations (5), (6), and (7) suggest that the existence of these points depends only on the signs of $q(\Delta,K)$ and $p_\pm(\Delta,K)$. This dependence leads to the following lemma (see Fig. 2).

Lemma 1. The necessary and sufficient condition for Δ and K to satisfy $q(\Delta,K) > 0$ is described by

$$q(\Delta,K) > 0 \Leftrightarrow$$
$$K \in \begin{cases} (K_1, +\infty) & \text{for } \Delta \in [0, \Delta_2], \\ (K_1, K_2) \cup (K_3, +\infty) & \text{for } \Delta \in [\Delta_2, +\infty). \end{cases} \tag{8}$$

[2]The previous work [54] also focused on the two crossing points to analyze the local stability of an equilibrium point in a single oscillator with delayed-feedback control.

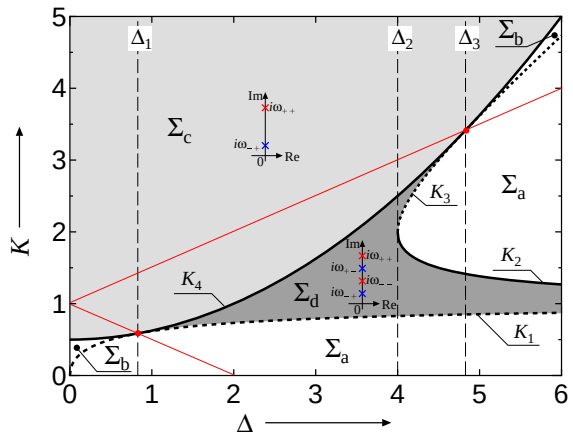

FIG. 2. Four regions $\Sigma_{a,b,c,d}$ in parameter space (Δ, K): for $\Sigma_{a,b}$, there does not exist any point on the imaginary axis; for Σ_c, there exist $i\omega_{++,-+}$; and for Σ_d, there exist $i\omega_{++,+-,--,-+}$ (see Lemmas 1 and 2).

Under $q(\Delta, K) > 0$, the necessary and sufficient conditions for Δ and K to satisfy $p_\pm(\Delta, K) > 0$ are given by

$$p_+(\Delta, K) > 0$$
$$\Leftrightarrow K \in \begin{cases} (K_4, +\infty) & \text{for } \Delta \in [0, \Delta_1], \\ (K_1, +\infty) & \text{for } \Delta \in [\Delta_1, \Delta_2], \\ (K_1, K_2) \cup (K_3, +\infty) & \text{for } \Delta \in [\Delta_2, \Delta_3], \\ (K_1, K_2) \cup (K_4, +\infty) & \text{for } \Delta \in [\Delta_3, +\infty), \end{cases} \tag{9}$$
$$p_-(\Delta, K) > 0$$
$$\Leftrightarrow K \in \begin{cases} (K_1, K_4) & \text{for } \Delta \in [\Delta_1, \Delta_2], \\ (K_1, K_2) \cup (K_3, K_4) & \text{for } \Delta \in [\Delta_2, \Delta_3], \\ (K_1, K_2) & \text{for } \Delta \in [\Delta_3, +\infty), \end{cases} \tag{10}$$

where $K_{1,2,3,4}$ and $\Delta_{1,2,3}$ are defined as

$$K_1 := \frac{-\Delta + \sqrt{\Delta^2 + 4\Delta}}{2}, \quad K_2 := \frac{+\Delta - \sqrt{\Delta^2 - 4\Delta}}{2},$$
$$K_3 := \frac{+\Delta + \sqrt{\Delta^2 - 4\Delta}}{2}, \quad K_4 := \frac{1 + \Delta^2/4}{2},$$
$$\Delta_1 := -2 + 2\sqrt{2}, \quad \Delta_2 := 4, \quad \Delta_3 := +2 + 2\sqrt{2}.$$

Proof. See Appendix A. ∎

This lemma and definition (5) indicate that crossing points $i\omega_{++,-+}$ ($i\omega_{++,+-,--,-+}$) can arise for all $\Delta \in [0, +\infty)$ [for all $\Delta \in [\Delta_1, +\infty)$] by choosing the appropriate K.

Now we turn our attention to the relation between the existence of these points and the parameter space (Δ, K). According to the positivity or negativity of $q(\Delta, K)$ and $p_\pm(\Delta, K)$, the parameter space (Δ, K) is divided into four regions, as follows (see Fig. 2):

$$\Sigma_a := \{(\Delta, K) \in \mathbb{R}_+^2 : q < 0\}$$
$$= \{(\Delta, K) : K \in [0, K_1) \cup (K_2, K_3), \ \Delta \in [0, +\infty)\},$$
$$\Sigma_b := \{(\Delta, K) \in \mathbb{R}_+^2 : q > 0, \ p_+ < 0, \ p_- < 0\}$$
$$= \Sigma_b^{(1)} \cup \Sigma_b^{(2)},$$
$$\Sigma_c := \{(\Delta, K) \in \mathbb{R}_+^2 : q > 0, \ p_+ > 0, \ p_- < 0\}$$
$$= \{(\Delta, K) : K \in (K_4, +\infty), \ \Delta \in [0, +\infty)\},$$
$$\Sigma_d := \{(\Delta, K) \in \mathbb{R}_+^2 : q > 0, \ p_+ > 0, \ p_- > 0\}$$
$$= \Sigma_d^{(1)} \cup \Sigma_d^{(2)} \cup \Sigma_d^{(3)},$$

where $\Sigma_b^{(1,2)}$ and $\Sigma_d^{(1,2,3)}$ are defined as

$$\Sigma_b^{(1)} := \{(\Delta, K) : K \in (K_1, K_4), \ \Delta \in [0, \Delta_1)\},$$
$$\Sigma_b^{(2)} := \{(\Delta, K) : K \in (K_3, K_4), \ \Delta \in (\Delta_3, +\infty)\},$$
$$\Sigma_d^{(1)} := \{(\Delta, K) : K \in (K_1, K_4), \ \Delta \in (\Delta_1, \Delta_2)\},$$
$$\Sigma_d^{(2)} := \{(\Delta, K) : K \in (K_1, K_2), \ \Delta \in [\Delta_2, +\infty)\},$$
$$\Sigma_d^{(3)} := \{(\Delta, K) : K \in (K_3, K_4), \ \Delta \in [\Delta_2, \Delta_3)\}.$$

The relations between regions $\Sigma_{a,b,c,d}$ and the existence of $i\omega_{++,+-,--,-+}$ are summarized by the following lemma.

Lemma 2. The relations between regions $\Sigma_{a,b,c,d}$ and crossing points $i\omega_{++,+-,--,-+}$ are described as follows: for $\Sigma_{a,b}$, there does not exist any point on the imaginary axis; for Σ_c, there exist $i\omega_{++,-+}$; and for Σ_d, there exist $i\omega_{++,+-,--,-+}$. Root s passing points $i\omega_{+-,-+}$ ($i\omega_{++,--}$) always moves from right (left) to left (right) with an increase in τ. Furthermore, these points have the following relation:

$$\omega_{++} > \omega_{+-} > \omega_{--} > \omega_{-+}. \tag{11}$$

Proof. It is obvious from the definitions of regions $\Sigma_{a,b,c,d}$ and frequencies $\omega_{++,+-,--,-+}$ that the regions and the crossing points have such relations. In order to determine the direction of the passing, with $g(s, \tau) = 0$ and Eq. (4), we have

$$\mathrm{Re}\left[\frac{ds}{d\tau}\right]_{s=i\omega} = \frac{\omega(\omega - \overline{\Omega})\{(1-K)^2 + (\omega - \overline{\Omega})^2 - \Delta^2/4\}}{\{-1 + K + K^2\tau\cos 2\omega\tau\}^2 + \{\omega - \overline{\Omega} - K^2\tau\sin 2\omega\tau\}^2}, \tag{12}$$

for regions $\Sigma_{c,d}$. The denominator of Eq. (12) is positive. Thus, from the sign of its numerator at $i\omega_{++,+-,--,-+}$, it is straightforward to see that the two inequalities

$$\mathrm{Re}\left[\frac{ds}{d\tau}\right]_{s=i\omega_{+-},i\omega_{-+}} < 0, \quad \mathrm{Re}\left[\frac{ds}{d\tau}\right]_{s=i\omega_{++},i\omega_{--}} > 0,$$

are always satisfied. These inequalities show that root s passing points $i\omega_{+-,-+}$ ($i\omega_{++,--}$) moves from right (left) to left (right) with an increase in τ. The magnitude relation between these points is obtained from the relation $p_+ > p_-$ in Eq. (6) and definition (5). ∎

We say that points $i\omega_{+-,-+}$ ($i\omega_{++,--}$) are stabilizing (destabilizing) points. These points are interlacing on the imaginary axis owing to relation (11), as illustrated in Fig. 1. It must be emphasized that Lemmas 1 and 2 do not depend on the nominal frequency $\overline{\Omega}$ and the delay time τ. The analytical results in these lemmas depend only on the frequency mismatch Δ and the coupling strength K.

Lemmas 1 and 2 show that, for small mismatch $\Delta \in [0, \Delta_1)$ with $\Delta_1 := -2 + 2\sqrt{2}$, there exist only the two crossing points $i\omega_{++,-+}$ for Σ_c, which can be observed

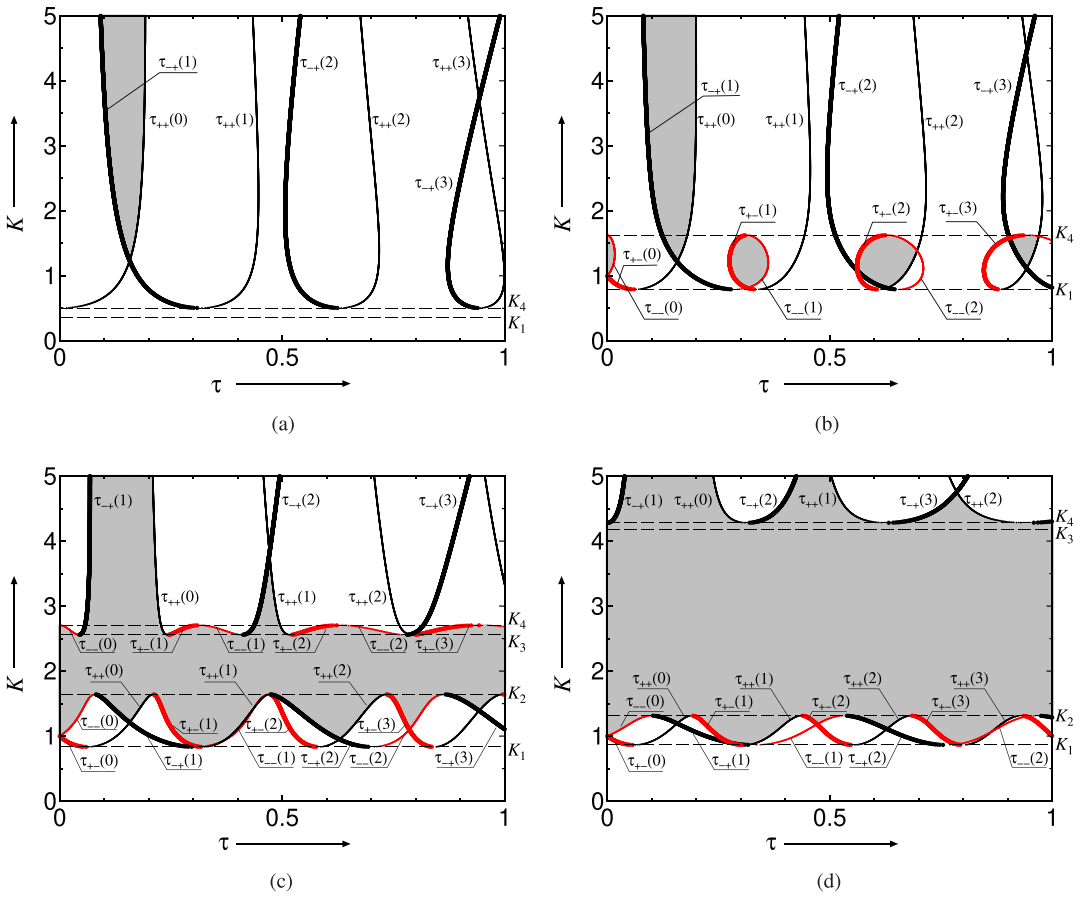

FIG. 3. Boundary curves and stability regions in coupling parameters space (τ, K) with $\overline{\Omega} = 10$ [$\tau_{-+(+-)}$: black (red) thick lines, $\tau_{++(--)}$: black (red) thin lines]: (a) $\Delta = 0.2 \in [0, \Delta_1)$, (b) $\Delta = 3.0 \in (\Delta_1, \Delta_2)$, (c) $\Delta = 4.2 \in (\Delta_2, \Delta_3)$, and (d) $\Delta = 5.5 \in (\Delta_3, +\infty)$. The boundary curves and the stability regions are analytically obtained in Lemma 3 and in Theorem 1, respectively.

even without mismatch $\Delta = 0$. On the other hand, for mismatch greater than Δ_1, there exist the four crossing points $i\omega_{++,+-,--,-+}$ for $\Sigma_{\rm d}$, which cannot be observed with $\Delta = 0$. This fact indicates that Δ_1 can be treated as the threshold of the frequency mismatch effect.

B. Boundary curves of stability

Let us consider the situation in which root s of $g(s, \tau)$ is located on the imaginary axis (see Fig. 1),

$$s(\tau_{++}) = i\omega_{++},\ s(\tau_{+-}) = i\omega_{+-},$$
$$s(\tau_{--}) = i\omega_{--},\ s(\tau_{-+}) = i\omega_{-+}. \tag{13}$$

This situation suggests that root s is passing one of points $i\omega_{++,+-,--,-+}$ at one of the corresponding delays, $\tau = \tau_{++,+-,--,-+}$. This subsection analytically provides the boundary curves of stability, the sets of coupling parameters (τ, K) at which root s is located on the imaginary axis, and shows that these curves can be classified into four types according to the frequency mismatch Δ.

For the four types of boundary curves, we consider some numerical examples with $\overline{\Omega} = 10$. The four types corresponding to mismatches $\Delta \in [0, \Delta_1)$, (Δ_1, Δ_2), (Δ_2, Δ_3), and $(\Delta_3, +\infty)$ are shown in Figs. 3(a), 3(b), 3(c), and 3(d), respectively. First, with mismatch $\Delta \in [0, \Delta_1)$, we have the following (see also Fig. 2). For $K < K_4$, root s does not cross the imaginary axis (i.e., boundary curves do not exist). For $K > K_4$, root s can cross the imaginary axis at $i\omega_{++,-+}$ (i.e., $\tau_{++,-+}$). These relations agree with the boundary curves for $\Delta \in [0, \Delta_1)$ plotted in Fig. 3(a). Second, with $\Delta \in (\Delta_1, \Delta_2)$, we have the following from Fig. 2. For $K < K_1$, root s never crosses the imaginary axis (i.e., boundary curves do not exist). For $K \in (K_1, K_4)$, root s can cross the imaginary axis at $i\omega_{++,+-,--,-+}$ (i.e., $\tau_{++,+-,--,-+}$). For $K > K_4$, root s can cross at $i\omega_{++,-+}$ (i.e., $\tau_{++,-+}$). These relations agree with the boundary curves for $\Delta \in (\Delta_1, \Delta_2)$ in Fig. 3(b). Third, with $\Delta \in (\Delta_2, \Delta_3)$, the following are obtained. For $K \in [0, K_1) \cup (K_2, K_3)$, root s never crosses the imaginary axis (i.e., boundary curves do not exist). For $K \in (K_1, K_2) \cup (K_3, K_4)$, root s can cross at $i\omega_{++,+-,--,-+}$ (i.e., $\tau_{++,+-,--,-+}$). For $K > K_4$, root s can cross at $i\omega_{++,-+}$ (i.e., $\tau_{++,-+}$). These relations agree with the boundary curves for $\Delta \in (\Delta_2, \Delta_3)$ in Fig. 3(c). Fourth, with $\Delta \in (\Delta_3, +\infty)$, the following are obtained. For $K \in [0, K_1) \cup (K_2, K_4)$, root s never crosses (i.e., boundary curves do not exist). For $K \in (K_1, K_2)$, root s can cross at $i\omega_{++,+-,--,-+}$ (i.e., $\tau_{++,+-,--,-+}$). For $K > K_4$, root s can cross at $i\omega_{++,-+}$ (i.e., $\tau_{++,-+}$). These relations agree with the boundary curves for $\Delta \in (\Delta_3, +\infty)$ in Fig. 3(d).

Boundary curves $\tau_{++,+-,--,-+}$ in Fig. 3 can be analytically obtained by the following lemma.

Lemma 3. The time delays $\tau_{++,+-,--,-+}$ in situation (13) are analytically provided as follows:
for $K \leqslant 1$,

$$\tau_{++}(l) := \frac{\psi_-/2 + l\pi}{\overline{\Omega} + \sqrt{p_+}}, \quad \tau_{+-}(l) := \frac{\psi_+/2 + l\pi}{\overline{\Omega} + \sqrt{p_-}},$$
$$\tau_{--}(l) := \frac{-\psi_+/2 + l\pi}{\overline{\Omega} - \sqrt{p_-}}, \quad \tau_{-+}(l) := \frac{-\psi_-/2 + l\pi}{\overline{\Omega} - \sqrt{p_+}},$$

for $K \geqslant 1$,

$$\tau_{++}(l) := \frac{\pi - \psi_-/2 + l\pi}{\overline{\Omega} + \sqrt{p_+}}, \quad \tau_{+-}(l) := \frac{-\psi_+/2 + l\pi}{\overline{\Omega} + \sqrt{p_-}},$$
$$\tau_{--}(l) := \frac{\psi_+/2 + l\pi}{\overline{\Omega} - \sqrt{p_-}}, \quad \tau_{-+}(l) := \frac{-\pi + \psi_-/2 + l\pi}{\overline{\Omega} - \sqrt{p_+}},$$

where

$$\psi_\pm := \cos^{-1} \frac{2(1-K)^2 \pm \sqrt{q(\Delta, K)}}{K^2} \in [0, \pi].$$

$l \in \mathbb{Z}$ is an integer.

Proof. See Appendix B. ∎

Note that time delays $\tau_{++,-+}$ (see black lines in Fig. 3) with no mismatch (i.e., with $\Delta = 0$) were analytically provided in previous studies [12,13]. However, delays $\tau_{+-,--}$ (see red lines in Fig. 3) induced by mismatch (i.e., with $\Delta > 0$) were not. Note also that the boundary curves of Fig. 3 are plotted by delays $\tau_{++,+-,--,-+}$ described in Lemma 3.

IV. DESIGN OF PARAMETERS INDUCING AMPLITUDE DEATH

The goal of this section is to design the coupling parameters and the frequency mismatch to induce amplitude death. To this end, we elucidate the behavior of root s in the complex plane by increasing delay τ from zero.

First, we concentrate on root s for the case of $\tau = 0$. The characteristic function (3) at $\tau = 0$, i.e., $g(s,\ 0)$, has two roots [6],

$$s = \begin{cases} 1 - K + i\left(\overline{\Omega} \pm \sqrt{\Delta^2/4 - K^2}\right) & (K \leqslant \Delta/2), \\ 1 - K \pm \sqrt{K^2 - \Delta^2/4} + i\overline{\Omega} & (K \geqslant \Delta/2). \end{cases} \tag{14}$$

According to these roots, (Δ, K) space can be divided into three regions, as shown in Fig. 4,

$$\Sigma_1 := \{(\Delta, K) : K \in [0, K_4) \cap [0, 1),\ \Delta \in [0, +\infty)\},$$
$$\Sigma_2 := \Sigma_c,$$
$$\Sigma_3 := \{(\Delta, K) : K \in (1, K_4),\ \Delta \in (2, +\infty)\}.$$

The relation between the roots and the regions is described by the following lemma.

Lemma 4. Consider two roots (14) of characteristic function (3) at $\tau = 0$. The signs of the real parts of these roots depend on three regions $\Sigma_{1,2,3}$ in (Δ, K) space, as follows. For Σ_1, the two roots have positive real parts. For Σ_2, one of the two roots has a positive real part and the other has a negative real part. For Σ_3, the two roots have negative real parts.

Proof. The real parts of the roots (14) clarify the relation between the roots at $\tau = 0$ and the regions. Thus, we omit the proof. ∎

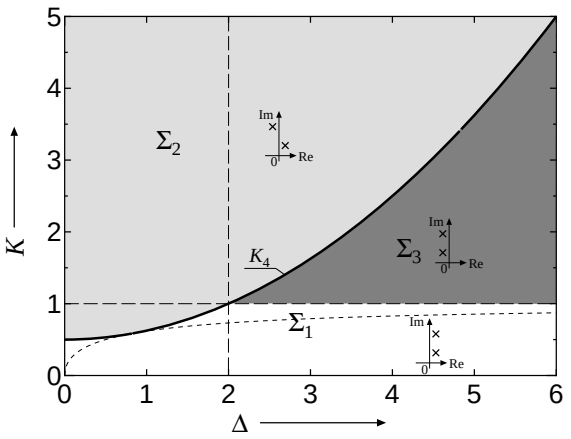

FIG. 4. Three regions $\Sigma_{1,2,3}$ in $(\Delta,\ K)$ space. For Σ_1 (Σ_3), the two roots of $g(s,\ 0)$ have positive (negative) real parts. For Σ_2, one of the two roots has a positive real part and the other has a negative real part (see Lemma 4).

Note that in the case of no delay, $\tau = 0$, amplitude death occurs at Σ_3. This was reported in a previous study [6].

Second, we examine the behavior of root s in the complex plane for $\tau \geqslant 0$. When the delay τ increases from zero, a root crosses one of points $i\omega_{++,+-,--,-+}$ at one of the corresponding delays, $\tau = \tau_{++,+-,--,-+}$. The existence of these points and the direction of the crossing over the imaginary axis were clarified in Lemma 2. Furthermore, the delays were analytically provided in Lemma 3. These results and Lemma 4 lead to the theorem described below.

As a preliminary to presenting the theorem, the numbers of each critical positive delay $\tau_{++,+-,--,-+}$ that are lower than a certain value of τ (i.e., the number of boundary curves existing on the left side of a certain value of τ in space (τ, K), as shown in Fig. 3) are described as follows (see Appendix C for more details):
for $K \leqslant 1$,

$$l^{(a)}_{++}(\tau) := \left\lfloor \frac{\overline{\Omega} + \sqrt{p_+}}{\pi}\tau - \frac{\psi_-}{2\pi} \right\rfloor + 1, \tag{15a}$$
$$l^{(a)}_{+-}(\tau) := \left\lfloor \frac{\overline{\Omega} + \sqrt{p_-}}{\pi}\tau - \frac{\psi_+}{2\pi} \right\rfloor + 1, \tag{15b}$$
$$l^{(a)}_{--}(\tau) := \left\lfloor \frac{\overline{\Omega} - \sqrt{p_-}}{\pi}\tau + \frac{\psi_+}{2\pi} \right\rfloor, \tag{15c}$$
$$l^{(a)}_{-+}(\tau) := \left\lfloor \frac{\overline{\Omega} - \sqrt{p_+}}{\pi}\tau + \frac{\psi_-}{2\pi} \right\rfloor, \tag{15d}$$

for $K \geqslant 1$,

$$l^{(b)}_{++}(\tau) := \left\lfloor \frac{\overline{\Omega} + \sqrt{p_+}}{\pi}\tau + \frac{\psi_-}{2\pi} \right\rfloor, \tag{16a}$$
$$l^{(b)}_{+-}(\tau) := \left\lfloor \frac{\overline{\Omega} + \sqrt{p_-}}{\pi}\tau + \frac{\psi_+}{2\pi} \right\rfloor, \tag{16b}$$
$$l^{(b)}_{--}(\tau) := \left\lfloor \frac{\overline{\Omega} - \sqrt{p_-}}{\pi}\tau - \frac{\psi_+}{2\pi} \right\rfloor + 1, \tag{16c}$$

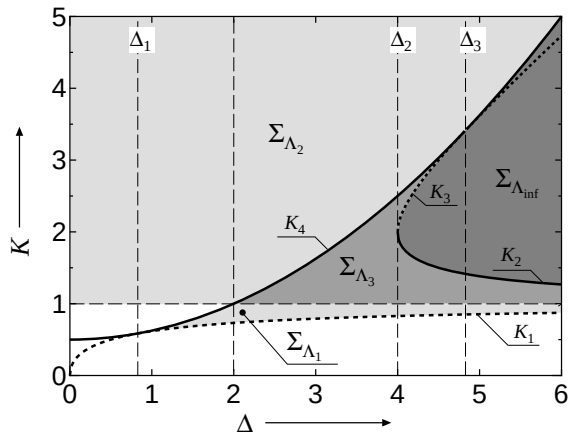

FIG. 5. Four regions, Σ_{Λ_1}, Σ_{Λ_2}, Σ_{Λ_3}, and $\Sigma_{\Lambda_{\rm inf}}$, in (Δ, K) space (see Theorem 1).

$$l^{(\rm b)}_{-+}(\tau) := \left\lfloor \frac{\overline{\Omega} - \sqrt{p_+}}{\pi}\tau - \frac{\psi_-}{2\pi} \right\rfloor + 1, \tag{16d}$$

where $\lfloor z \rfloor$ denotes the largest integer that is not greater than $z \in \mathbb{R}$. Furthermore, the delay intervals based on $l^{(\rm a),(\rm b)}_{++,+-,--,-+}(\tau)$ are defined as

$$\Lambda_1 := \{\tau \geqslant 0 : l^{(\rm a)}_{+-}(\tau) + l^{(\rm a)}_{-+}(\tau) = l^{(\rm a)}_{++}(\tau) + l^{(\rm a)}_{--}(\tau) + 2\}, \tag{17a}$$

$$\Lambda_2 := \{\tau \geqslant 0 : l^{(\rm b)}_{-+}(\tau) = l^{(\rm b)}_{++}(\tau) + 1\}, \tag{17b}$$

$$\Lambda_3 := \{\tau \geqslant 0 : l^{(\rm b)}_{+-}(\tau) + l^{(\rm b)}_{-+}(\tau) = l^{(\rm b)}_{++}(\tau) + l^{(\rm b)}_{--}(\tau)\}. \tag{17c}$$

In addition, the four regions in space (Δ, K) (see Fig. 5) are given by

$$\Sigma_{\Lambda_1} := \Sigma_{\rm d} \cap \Sigma_{K<1}, \quad \Sigma_{\Lambda_2} := \Sigma_{\rm c} \cap \Sigma_{K>1},$$
$$\Sigma_{\Lambda_3} := \Sigma_{\rm d} \cap \Sigma_{K>1}, \quad \Sigma_{\Lambda_{\rm inf}} := \Sigma^{(1)}_{\Lambda_{\rm inf}} \cup \Sigma^{(2)}_{\Lambda_{\rm inf}},$$

where

$$\Sigma_{K<1} := \{(\Delta, K) : K \in [0, 1),\ \Delta \in [0, +\infty)\},$$
$$\Sigma_{K>1} := \{(\Delta, K) : K \in (1, +\infty),\ \Delta \in [0, +\infty)\},$$
$$\Sigma^{(1)}_{\Lambda_{\rm inf}} := \{(\Delta, K) : K \in (K_2, K_3),\ \Delta \in (\Delta_2, \Delta_3]\},$$
$$\Sigma^{(2)}_{\Lambda_{\rm inf}} := \{(\Delta, K) : K \in (K_2, K_4),\ \Delta \in (\Delta_3, +\infty)\}.$$

The above definitions and Lemmas 2, 3, and 4 are summarized as the following theorem.

Theorem 1. The equilibrium point $Z^*_1 = Z^*_2 = 0$ of delay-coupled oscillators (1) is locally stable for τ belonging to the following intervals:

$$\tau \in \begin{cases} \Lambda_1 & \text{for } (\Delta, K) \in \Sigma_{\Lambda_1}, \\ \Lambda_2 & \text{for } (\Delta, K) \in \Sigma_{\Lambda_2}, \\ \Lambda_3 & \text{for } (\Delta, K) \in \Sigma_{\Lambda_3}, \\ [0, +\infty) & \text{for } (\Delta, K) \in \Sigma_{\Lambda_{\rm inf}}. \end{cases}$$

Proof. See Appendix D. ∎

This theorem allows us to design (Δ, K, τ) analytically such that $Z^*_1 = Z^*_2 = 0$ is locally stable. From regions Σ_{Λ_1}, Σ_{Λ_2}, Σ_{Λ_3}, and $\Sigma_{\Lambda_{\rm inf}}$ illustrated in Fig. 5, we note the following.

(i) Without mismatch $\Delta = 0$ or with small mismatch $\Delta \in (0, \Delta_1)$ (see Σ_{Λ_2}), amplitude death cannot be induced for K less than 1.

(ii) With mismatch $\Delta > \Delta_1$ (see Σ_{Λ_1}), amplitude death can be induced, even by K less than 1 [see Fig. 3(b)].

(iii) For the sum set of Σ_{Λ_3}, $\Sigma_{\Lambda_{\rm inf}}$, K_2, and K_3 (i.e., Σ_3), amplitude death can be induced, even without delay $\tau = 0$ [see Figs. 3(c) and 3(d)].

(iv) For $\Sigma_{\Lambda_{\rm inf}}$, amplitude death can be induced with all $\tau \geqslant 0$ [see Figs. 3(c) and 3(d)].

Here we comment on the notable observations. For observation (ii), the mismatch can be useful to reduce the coupling strength (i.e., the lowest $K = 1 \to K = K_1 < 1$). For observation (iv), amplitude death can be robust against delay $\tau \geqslant 0$: this corresponds to the concept of delay-independent stability in the field of control theory [51]. In addition, we discuss observation (iv) from the viewpoint of long-delay systems [55]. For $\Delta \in (\Delta_2, \Delta_3)$ [$\Delta \in (\Delta_3, +\infty)$], the stability region between K_2 and K_3 (K_2 and K_4) as shown in Fig. 3(c) [Fig. 3(d)] exists even for sufficiently large delay τ. The reason is described below. Note that the stability region corresponds to the region $\Sigma_{\Lambda_{\rm inf}}$, which is a subset of $\Sigma_{\rm a} \cup \Sigma_{\rm b}$ (see Figs. 2 and 5). Since crossing points for $\Sigma_{\rm a} \cup \Sigma_{\rm b}$ do not exist (see Lemma 2), for $\Sigma_{\Lambda_{\rm inf}}$, root s never crosses the imaginary axis for any delay τ. Thus, the stability at $\tau = 0$ (see Lemma 4 and Σ_3 in Fig. 4) remains for all $\tau \geqslant 0$. In other words, if one wants to induce amplitude death in long-delay systems, (Δ, K) should be located in $\Sigma_{\Lambda_{\rm inf}}$.

Let us consider two numerical examples. For a given mismatch Δ (strength K), the delay τ and the strength K (the mismatch Δ) are designed according to Lemma 3 and Theorem 1. As a first example, for given mismatches $\Delta = 0.2$, $\Delta = 3.0$, $\Delta = 4.2$, and $\Delta = 5.5$, we design τ and K. The time delays $\tau_{++,+-,--,-+}$ described in Lemma 3 and the delay intervals (17) are plotted in space (τ, K) when K increases from zero. Note that, instead of plotting the delay intervals (17), we also easily obtain the stability regions using the following two pieces of information:[3] the directions of root s crossing the imaginary axis as provided in Lemma 2 and the number of unstable roots at $\tau = 0$ as given in Lemma 4. Figure 3 shows the critical delays (i.e., black and red curves) and the intervals (i.e., gray regions) for $\Delta = 0.2$, $\Delta = 3.0$, $\Delta = 4.2$, and $\Delta = 5.5$. If τ and K are chosen from the gray regions, it is guaranteed that $Z^*_1 = Z^*_2 = 0$ of delay-coupled oscillators (1) is locally stable. As a second example, for a given strength $K = 1.5$, the critical delays $\tau_{++,+-,--,-+}$ of Lemma 3 and the intervals (17) are plotted in space (τ, Δ) when Δ increases from zero, as shown in Fig. 6. These numerical examples suggest that the boundary curves and the stability regions can be easily obtained analytically using Lemma 3 and Theorem 1.

Here, we turn our attention to attractive examples. Figures 7(a) and 7(b) show the color plots for the real part of

[3]This concept, a well-known approach in the control community [50–53], is used in the proof of Theorem 1 (i.e., Appendix D).

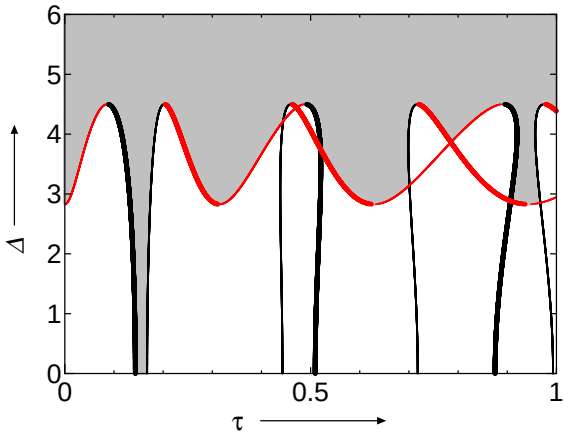

FIG. 6. Boundary curves and stability regions with $\overline{\Omega} = 10$ in coupling parameters space (τ, Δ) for a given $K = 1.5$. These curves and the stability regions are analytically obtained in Lemma 3 and in Theorem 1, respectively.

the rightmost roots[4] of $g(s, \tau)$ with $\Delta = 1.9$ in (τ, K) space for $\overline{\Omega} = 5$ and for $\overline{\Omega} = 10$, respectively. The areas filled with color denote the parameter sets in which the real part is negative: the colored areas agree with the stability regions obtained in Theorem 1. Furthermore, Theorem 1 and Fig. 5 indicate that, for $\Delta \in (\Delta_1, 2)$, the stability regions are separated into upper regions (i.e., $K > 1$) and lower regions (i.e., $K < 1$). The upper regions can be seen even in the absence of the mismatch (i.e., $\Delta = 0$) [6]. In contrast, the lower regions appear only in the presence of the mismatch. For $\overline{\Omega} = 5$, as shown in Fig. 7(a) (see the color of the inset), the parameter range of the lower region is narrow compared to the upper region. However, the stability of the lower region is stronger than that of the upper region. For $\overline{\Omega} = 10$, as shown in Fig. 7(b), the stability of the lower region is not so weak compared to that of the upper region. These interesting examples and Theorem 1 suggest that amplitude death can be induced with small K and with strong stability if Δ, K, and τ are designed such that $\tau \in \Lambda_1$ for $(\Delta, K) \in \Sigma_{\Lambda_1}$ holds. Note that our results can analytically provide the stability regions but not the strength of the stability. Further insight into the analytical treatment of the strength is left for a future study. Here, from Figs. 3(b) and 7 with the nominal frequency $\overline{\Omega} = 5$ or 10, for $\Delta \in (\Delta_1, \Delta_2)$, we observe that there exist two types of amplitude death islands: the smaller-size islands periodically occur several times with respect to τ, but the larger-size island occurs only once. However, for the higher nominal frequency (e.g., $\overline{\Omega} = 20$ or 30), we have observed that both islands occur periodically several times.

V. EXTENSION TO COMPLETE BIPARTITE NETWORKS

This section shows that the analytical results obtained in the preceding section can be extended to delay-coupled oscillator networks with complete bipartite topologies (see Fig. 8).

[4]The rightmost roots are numerically obtained by the function `eigAM` [56] in MATLAB.

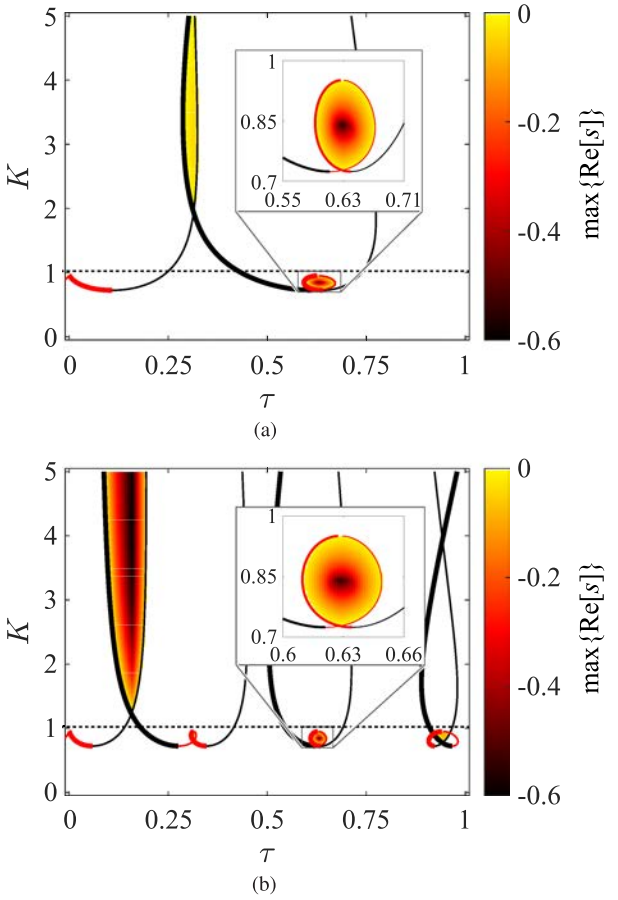

FIG. 7. Real part of rightmost roots with $\Delta = 1.9$ in (τ, K) space for (a) $\overline{\Omega} = 5$ and (b) $\overline{\Omega} = 10$. The white areas represent the parameter sets with the positive real part.

Consider the delay-coupled oscillator networks

$$\dot{Z}_j(t) = \{1 + i\Omega_1 - |Z_j(t)|^2\}Z_j(t) + K\left\{\frac{1}{n_2}\sum_{k=n_1+1}^{n_1+n_2} Z_k(t-\tau) - Z_j(t)\right\}, \quad (18)$$

for $j = 1, \ldots, n_1$,

$$\dot{Z}_j(t) = \{1 + i\Omega_2 - |Z_j(t)|^2\}Z_j(t) + K\left\{\frac{1}{n_1}\sum_{k=1}^{n_1} Z_k(t-\tau) - Z_j(t)\right\}, \quad (19)$$

for $j = n_1 + 1, \ldots, n_1 + n_2$, where $n_1 \geqslant 1$ and $n_2 \geqslant 1$ are the numbers of oscillators with frequencies Ω_1 and Ω_2, respectively. The networks (18) and (19) have complete bipartite topologies, i.e., every oscillator with Ω_1 is connected to every oscillator with Ω_2, as illustrated in Fig. 8.

The oscillator networks have the equilibrium point

$$Z_j^* = 0, \forall j \in \{1, \ldots, n_1 + n_2\}. \quad (20)$$

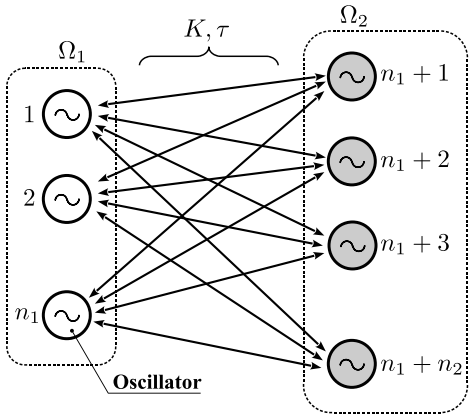

FIG. 8. A sketch of delay-coupled oscillator networks with a complete bipartite topology: every oscillator with Ω_1 $(1, \ldots, n_1)$ is connected to every oscillator with Ω_2 $(1, \ldots, n_2)$.

The linearized dynamics of the networks at equilibrium point (20),

$$\begin{bmatrix}\dot{\boldsymbol{z}}_1(t)\\ \dot{\boldsymbol{z}}_2(t)\end{bmatrix} = \begin{bmatrix}a_1\boldsymbol{I}_{n_1} & \boldsymbol{0}\\ \boldsymbol{0} & a_2\boldsymbol{I}_{n_2}\end{bmatrix}\begin{bmatrix}\boldsymbol{z}_1(t)\\ \boldsymbol{z}_2(t)\end{bmatrix} + \begin{bmatrix}\boldsymbol{0} & (K/n_2)\boldsymbol{1}_{n_1\times n_2}\\ (K/n_1)\boldsymbol{1}_{n_2\times n_1} & \boldsymbol{0}\end{bmatrix}\begin{bmatrix}\boldsymbol{z}_1(t-\tau)\\ \boldsymbol{z}_2(t-\tau)\end{bmatrix}, \tag{21}$$

has the parameters

$$a_{1,2} := 1 - K + i\Omega_{1,2}. \tag{22}$$

The state variables $\boldsymbol{z}_1(t) := [z_1(t) \cdots z_{n_1}(t)]^{\mathrm{T}}$ and $\boldsymbol{z}_2(t) := [z_{n_1+1}(t) \cdots z_{n_1+n_2}(t)]^{\mathrm{T}}$ consist of small perturbations around equilibrium point (20), $z_j(t) := Z_j(t) - Z_j^*$, $\forall j \in \{1, \ldots, n_1+n_2\}$. The symbol $\boldsymbol{1}_{n\times m}$ denotes an $n \times m$ ones matrix. The stability of linear system (21), which is equivalent to the local stability of equilibrium point (20) of the networks, is governed by the characteristic function

$$G(s) = \det\begin{bmatrix}(s-a_1)\boldsymbol{I}_{n_1} & -(K/n_2)\mathrm{e}^{-s\tau}\boldsymbol{1}_{n_1\times n_2}\\ -(K/n_1)\mathrm{e}^{-s\tau}\boldsymbol{1}_{n_2\times n_1} & (s-a_2)\boldsymbol{I}_{n_2}\end{bmatrix}. \tag{23}$$

The function (23) and Theorem 1 yield the following simple result.

Corollary 1. Equilibrium point (20) of delay-coupled oscillator networks (18) and (19) under $n_1 + n_2 \geqslant 3$ is locally stable for τ belonging to the following intervals:

$$\tau \in \begin{cases}\Lambda_2 & \text{for } (\Delta, K) \in \Sigma_{\Lambda_2},\\ \Lambda_3 & \text{for } (\Delta, K) \in \Sigma_{\Lambda_3},\\ [0, +\infty) & \text{for } (\Delta, K) \in \Sigma_{\Lambda_{\mathrm{inf}}}.\end{cases}$$

Proof. Some facts on determinants [57] can be used to simplify function (23) as follows:

$$\begin{aligned}G(s) &= (s-a_1)^{n_1}\\ &\quad \det\left[(s-a_2)\boldsymbol{I}_{n_2} - \frac{K^2\mathrm{e}^{-2s\tau}}{n_1n_2(s-a_1)}\boldsymbol{1}_{n_2\times n_1}\boldsymbol{I}_{n_1}\boldsymbol{1}_{n_1\times n_2}\right]\\ &= (s-a_1)^{n_1}(s-a_2)^{n_2}\\ &\quad \det\left[\boldsymbol{I}_{n_2} - \frac{K^2\mathrm{e}^{-2s\tau}}{n_2(s-a_1)(s-a_2)}\boldsymbol{1}_{n_2\times n_2}\right]\end{aligned}$$

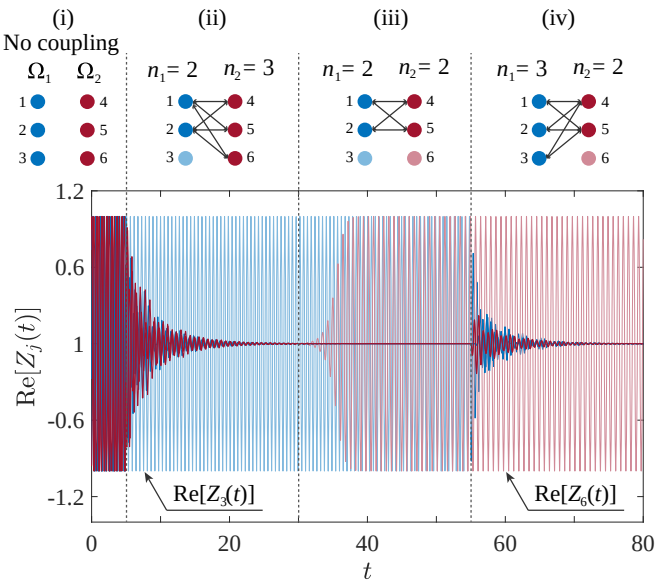

FIG. 9. Time series data of $\mathrm{Re}[Z_j(t)]$ on complete bipartite topologies ($\overline{\Omega} = 10$, $\Delta = 3.0$, $\tau = 0.65$, $K = 1.30$). The numbers of oscillators with Ω_1 and Ω_2 are changed over time as shown at the top.

$$\begin{aligned}&= (s-a_1)^{n_1}(s-a_2)^{n_2}\left\{1 - \frac{K^2\mathrm{e}^{-2s\tau}}{(s-a_1)(s-a_2)}\right\}\\ &= (s-a_1)^{n_1-1}(s-a_2)^{n_2-1}g(s).\end{aligned} \tag{24}$$

The analytical results for function $g(s)$ given by Eq. (3) were provided in the preceding section. Function $(s-a_1)^{n_1-1}(s-a_2)^{n_2-1}$ with Eq. (22) under $n_1 + n_2 \geqslant 3$ has at least one of the roots $s = 1 - K + i\Omega_{1,2}$. These roots are stable if and only if $K > 1$. As a consequence, Theorem 1 is not valid for the region with $K \leqslant 1$, which is the sum of Σ_{Λ_1} and $K = 1$. However, the other regions are still valid for networks (18) and (19).

This corollary indicates that, except for region Σ_{Λ_1}, Theorem 1 can be used to design the coupling parameters for inducing amplitude death in networks (18) and (19). In addition, note that the boundary curves $\tau_{++,+-,--,-+}$ provided in Lemma 3 are still valid, because they are based on $g(s)$ included in Eq. (24). It should be noted that Corollary 1 does not depend on the number of oscillators under $n_1 + n_2 \geqslant 3$. Thus, if the coupling parameters are designed with this corollary, then amplitude death can remain, even when some oscillators are deleted or added under $n_1 + n_2 \geqslant 3$.

Let us demonstrate a numerical example of delay-coupled oscillator networks with complete bipartite topologies. In order to confirm Corollary 1 on numerical simulations, this example deals with the networks, in which some oscillators are deleted or added (i.e., n_1 and n_2 are changed with time). The nominal frequency is fixed at $\overline{\Omega} = 10$ and the frequency mismatch is given as $\Delta = 3.0$. The delays $\tau_{++,+-,--,-+}$ for $K > 1$ in Lemma 3 and the intervals $\Lambda_{2,3}$ are plotted in space (τ, K) with an increase in K from 1. These plots can be seen in Fig. 3(b) for $K > 1$. For $K < 1$, Corollary 1 shows that amplitude death never occurs in the networks. The coupling parameters are set to $\tau = 0.65$ and $K = 1.30$ in this example.

Figure 9 shows time series data of the oscillator network. As shown at the top of Fig. 9, the numbers of oscillators with Ω_1 and Ω_2 are varied in time as follows: for (i) $t \in [0, 5)$, $n_1 = 0$ and $n_2 = 0$ (the oscillators are uncoupled), for (ii) $t \in [5, 30)$, $n_1 = 2$ and $n_2 = 3$, for (iii) $t \in [30, 55)$, $n_1 = 2$ and $n_2 = 2$, and for (iv) $t \in [55, 80]$, $n_1 = 3$ and $n_2 = 2$. The color of the time series data corresponds to that of the oscillators shown at the top. Even if n_1 and n_2 are changed with time, amplitude death is maintained, while deleted oscillators from the network [i.e., oscillator 3 in (ii) and (iii), and oscillator 6 in (iii) and (iv)] behave in an oscillatory manner. These data agree with Corollary 1.

VI. DISCUSSION

This section briefly clarifies the relation of the present paper to related previous studies and discusses the possibility of using our analytical results for thermoacoustic systems.

We dealt with the delay-induced amplitude death in oscillators that have frequency mismatch, but do not have other mismatches. The influences of several mismatches, except for frequency mismatch, on amplitude death were investigated. Thakur, Sharma, and Sen have considered oscillator networks with amplitude mismatch: the networks consist of inactive oscillators with zero amplitude and active oscillators with nonzero amplitude [58]. Zou *et al.* focused on oscillators with coupling-strength mismatch: the coupling strength depends on the coupling direction [59,60]. Furthermore, the following oscillators with delay time mismatches were considered: globally coupled oscillators, in which some of the oscillators are coupled by a delay connection and other oscillators are coupled by a nondelay connection [22]; Cartesian product oscillator networks consisting of two subnetworks, each of which has a different delay [61]; and tree-graph oscillator networks having asymmetric connection delays [47]. These previous studies on delay-induced amplitude death did not deal with frequency mismatch. In contrast, Zou, Zhan, and Kurths investigated the effect of frequency mismatch on amplitude death, but time delays were not included in connections (i.e., amplitude death induced by nondelay connections) [62]. In conclusion, the analytical treatment of amplitude death both with frequency mismatch and with delayed coupling remained an open research problem.

In the present paper, we analytically investigated amplitude death both with frequency mismatch and with delayed coupling. Frequency mismatch is one of the most important and fundamental mismatches. Delayed coupling is the natural diffusive connection with finite-speed propagation of information. Therefore, our analytical results can contribute to the development of the stability analysis reported in previous studies on delay-induced amplitude death. In addition, our analytical results may provide useful knowledge of how to make positive use of frequency mismatch for the following purposes: (i) enlargement of the stability regions, (ii) reduction of the coupling strength [see the stability regions in Figs. 3(b) and 7], or (iii) increase of the delay time [see also the stability regions in Figs. 3(b) and 7]. Such knowledge might be applied to suppress undesired oscillations that emerge in thermoacoustic systems. For (i), the enlargement of the stability regions is useful for systems to be robust against parameter shifts and errors. For (ii), the reduction of the coupling strength suggests that the diameter of the pipes or tubes for connecting thermoacoustic oscillators can be reduced. For (iii), the increase of the delay time means that the length of these pipes or tubes can be extended. As it has been well known that amplitude death often occurs with a strong coupling strength and short delays, the features in (ii) and (iii) could contribute to a wide range of choices for diameter and length.

The following are the limitations of the present paper. Although we were able to analytically obtain the effects of frequency mismatch on the delay-induced amplitude death, these results were valid only for a pair of oscillators and for oscillator networks with complete bipartite topologies. For our results to be applied to various situations, future research should extend our results to oscillator networks with other topologies, such as ring, path, and scale-free topologies. On the other hand, it is interesting to analytically derive the stability boundaries and regions in (Δ, K) space for a fixed τ. However, the key factor of the present paper, which is based on the four crossing points corresponding to the critical delay times (i.e., Lemmas 2 and 3), cannot be directly used to derive them in (Δ, K) space due to the fixity of τ.

VII. CONCLUSIONS

The present paper has analytically dealt with the stability of the equilibrium point within a pair of Stuart-Landau oscillators coupled by a delay connection. The relation of the frequency mismatch and the coupling strength with the stabilizing and destabilizing points located on the imaginary axis was revealed. The directions of the roots crossing these points and the delays at these points were analytically provided. These analytical results and delays that are shorter than a certain delay permit the design of the coupling parameters and frequency mismatch for amplitude death. Furthermore, it was demonstrated that we can induce amplitude death with strong stability by weak coupling if the frequency mismatch and the delay time are appropriately designed. In addition, we showed that the parts of analytical results for the pair of oscillators can be extended to delay-coupled oscillator networks with complete bipartite topologies.

ACKNOWLEDGMENTS

The present study was supported in part by JSPS KAKENHI (Grants No. 21H03513 and No. 20K19881).

APPENDIX A: PROOF OF LEMMA 1

This proof deals with the following three conditions: (i) $q(\Delta, K) > 0$, (ii) $p_+(\Delta, K) > 0$, and (iii) $p_-(\Delta, K) > 0$. For condition (i), we can rewrite $q(\Delta, K) > 0$ as

$$(K - K_{-1})(K - K_1)(K - K_2)(K - K_3) > 0, \tag{A1}$$

where $K_{-1} := -(\Delta + \sqrt{\Delta^2 + 4\Delta})/2$. We have nonpositive real $K_{-1} \leqslant 0$ for $\Delta \geqslant 0$, non-negative real $K_1 - 0$ for $\Delta \geqslant 0$, positive real $K_{2,3} > 0$ for $\Delta \geqslant \Delta_2$, and nonreal $K_{2,3}$ for $\Delta < \Delta_2$. Then, a property of the left-hand side of inequality (A1), a polynomial in K of degree 4, allows us to see that the

condition for (Δ, K) to satisfy inequality (A1) is described by Eq. (8).

For condition (ii), we deal with $p_+(\Delta, K) > 0$, which is equivalent to

$$(1-K)^2 - \frac{\Delta^2}{4} < \sqrt{K^4 - (1-K)^2\Delta^2}, \tag{A2}$$

under $q(\Delta, K) > 0$. Let us consider the following two cases: (ii-a) the left-hand side of inequality (A2) is negative or zero (i.e., $1 - \Delta/2 \leqslant K \leqslant 1 + \Delta/2$, which corresponds to the closed region bounded by the two red lines illustrated in Fig. 2); (ii-b) it is positive or zero (i.e., $K \leqslant 1 - \Delta/2$ or $K \geqslant 1 + \Delta/2$, which corresponds to the closed region under the lower red line or the closed region over the upper red line). For case (ii-a), inequality (A2) (i.e., $p_+(\Delta, K) > 0$) always holds. This is because its right-hand side is positive real for all (Δ, K) satisfying $q(\Delta, K) > 0$ [i.e., Eq. (8)]. Then, for case (ii-a) (i.e., the closed region bounded by the two red lines), the necessary and sufficient condition for (Δ, K) to satisfy $p_+(\Delta, K) > 0$ is described by Eq. (8). For case (ii-b) with $q(\Delta, K) > 0$, inequality (A2) can be written as $f(\Delta, K) > 0$, where

$$f(\Delta, K) := (K - K_4)\big(2K^2 - 2K + 1 + \Delta^2/4\big). \tag{A3}$$

The second factor of the right-hand side of Eq. (A3) is positive for all (Δ, K). Then, $f(\Delta, K) > 0$ is equivalent to

$$K > K_4.$$

Let us reconsider case (ii-b) for $K \leqslant 1 - \Delta/2$ and for $K \geqslant 1 + \Delta/2$. For $K \leqslant 1 - \Delta/2$ (see the region below the lower red line), it is easily seen that, with $\Delta \in [0, \Delta_1]$, there exists K such that both $f(\Delta, K) > 0$ and $K \leqslant 1 - \Delta/2$ hold. For $K \geqslant 1 + \Delta/2$ (see the region above the upper red line), we see that, with $\Delta \in [\Delta_3, +\infty)$, there exists K such that both $f(\Delta, K) > 0$ and $K \geqslant 1 + \Delta/2$ hold. As a result, we can say that, for case (ii-b), the condition for (Δ, K) to satisfy $f(\Delta, K) > 0$ is described by $K > K_4$ with $\Delta \in [0, \Delta_1]$ and $\Delta \in [\Delta_3, +\infty)$. These discussions are summarized by condition (9).

For condition (iii), $p_-(\Delta, K) > 0$, which is equivalent to

$$\frac{\Delta^2}{4} - (1-K)^2 > \sqrt{K^4 - (1-K)^2\Delta^2}, \tag{A4}$$

is dealt with under $q(\Delta, K) > 0$. The following two cases are considered: (iii-a) the left-hand side of inequality (A4) is negative (i.e., $K < 1 - \Delta/2$ or $K > 1 + \Delta/2$, which corresponds to the regions below the lower red line or above the upper red line illustrated in Fig. 2); (iii-b) it is positive or zero (i.e., $1 - \Delta/2 \leqslant K \leqslant 1 + \Delta/2$, which corresponds to the closed region bounded by the two red lines). For case (iii-a), inequality (A4) [i.e., $p_-(\Delta, K) > 0$] never holds, because the right-hand side is positive real for all (Δ, K) satisfying $q(\Delta, K) > 0$ [i.e., Eq. (8)]. Thus, there does not exist (Δ, K) satisfying inequality (A4) outside the closed region bounded by the two red lines. For case (iii-b) (i.e., the closed region bounded by the two red lines) with $q(\Delta, K) > 0$, inequality (A4) can be written as $f(\Delta, K) < 0$. The second factor of the right-hand side of Eq. (A3) is positive for all (Δ, K). Then, $f(\Delta, K) < 0$ is equivalent to

$$K < K_4. \tag{A5}$$

It is straightforward to see that, with $\Delta \in [\Delta_1, \Delta_3]$, there exists K such that both inequalities (A5) and $1 - \Delta/2 \leqslant K \leqslant 1 + \Delta/2$ hold. Thus, the condition for (Δ, K) to satisfy $f(\Delta, K) < 0$ is $K < K_4$ and $q(\Delta, K) > 0$ with $\Delta \in [\Delta_1, \Delta_3]$. The discussions on case (iii-b) are summarized by condition (10).

APPENDIX B: PROOF OF LEMMA 3

This proof analytically derives the critical delay τ_{++} satisfying Eq. (13) [i.e., $s(\tau_{++}) = i\omega_{++}$]. Substituting $\tau = \tau_{++}$ and $\omega = \omega_{++}$ defined in Eq. (5) into Eq. (4a) yields

$$2\omega_{++}\tau_{++} = \begin{cases} 2l\pi + \psi_-, & \text{(B1a)} \\ 2l\pi + 2\pi - \psi_-, & \text{(B1b)} \end{cases}$$

for $l \in \mathbb{Z}_0^+$. Furthermore, ω_{++} and τ_{++} satisfy Eq. (4b),

$$2(1-K)(\omega_{++} - \overline{\Omega}) = K^2 \sin 2\omega_{++}\tau_{++}. \tag{B2}$$

For $K \leqslant 1$ ($K \geqslant 1$), the sign of the left-hand side of Eq. (B2) allows us to see that Eq. (B1a) [Eq. (B1b)] holds, but Eq. (B1b) [Eq. (B1a)] does not hold. As a result, τ_{++} in Lemma 3 can be given by Eq. (B1a) for $K \leqslant 1$ and Eq. (B1b) for $K \geqslant 1$ with $\omega_{++} := \overline{\Omega} + \sqrt{p_+}$ defined in Eq. (5). A similar procedure is valid for the other critical delays $\tau_{+-,--,-+}$. As such, the derivations for the other delays are omitted in this proof.

APPENDIX C: DERIVATIONS OF THE NUMBERS OF CRITICAL DELAYS

Let us focus on the derivation of $l_{++}^{(a)}(\tau)$ in Eq. (15a). The largest integer l satisfying $\tau_{++}(l) < \tau$ is described by

$$l = l_{\max} := \left\lfloor \frac{\overline{\Omega} + \sqrt{p_+}}{\pi}\tau - \frac{\psi_-}{2\pi} \right\rfloor.$$

Since $\tau_{++}(-1) < 0$ and $\tau_{++}(0) > 0$ hold, we see that the leftmost positive critical delay in (τ, K) space is $\tau_{++}(0)$. Hence, the critical positive delays that are less than a certain value of τ are given by

$$\tau_{++}(l), \ \ l \in \{0, \ldots, l_{\max}\}.$$

As a result, the number of delays is described by Eq. (15a). A similar derivation can be used for the other numbers of delays in Eqs. (15) and (16).

APPENDIX D: PROOF OF THEOREM 1

This proof considers the behavior of the roots of the characteristic function $g(s, \tau)$ when τ increases from zero. We now focus on the three regions, $\Sigma_{1,2,3}$, illustrated in Fig. 4.

First, for the region Σ_2 ($=\Sigma_c$), Lemma 4 shows that $g(s, 0)$ at $\tau = 0$ has one root with a positive real part and another root with a negative real part. In addition, for region Σ_c ($=\Sigma_2$), Lemma 2 shows that, when τ increases from zero, the root with the positive real part passes the stabilizing point $i\omega_{-+}$ at $\tau = \tau_{-+}$ from right to left and then returns to the right via the destabilizing point $i\omega_{++}$ at $\tau = \tau_{++}$. Here, we focus on the numbers of positive τ_{-+} and τ_{++} that are lower than a certain

value of τ. It is easy to see that, if the number of positive τ_{-+} [i.e., $l^{(a)}_{-+}(\tau)$ or $l^{(b)}_{-+}(\tau)$] is equal to the sum of the number of unstable roots at $\tau = 0$ (i.e., 1) and the number of τ_{++} [i.e., $l^{(a)}_{++}(\tau)$ or $l^{(b)}_{++}(\tau)$], then we do not have unstable roots at the specific value of τ. Note that, for $K \leqslant 1$, there does not exist τ satisfying this relation, because the leftmost positive τ_{-+} and τ_{++} satisfy $\tau_{-+}(1) > \tau_{++}(0)$ and the periods of τ_{-+} and τ_{++} have the relation $\pi/(\overline{\Omega} - \sqrt{p_+}) > \pi/(\overline{\Omega} + \sqrt{p_+})$. Consequently, note that $g(s, \tau)$ for $(\Delta, K) \in \Sigma_{\Lambda_2}$, which is the product set of Σ_c ($=\Sigma_2$) and $\Sigma_{K>1}$, is stable (i.e., $Z_1^* = Z_2^* = 0$ is locally stable) for τ belonging to Λ_2, which is the set of τ satisfying this relation.

Second, for the region Σ_1, we see from Lemmas 4 and 2 that $g(s, 0)$ has two unstable roots. For region Σ_d, there exist stabilizing points $i\omega_{-+,+-}$ and destabilizing points $i\omega_{++,--}$, but for $\Sigma_{a,b}$, no points exist. Hence, we only have to consider region Σ_{Λ_1}, which is the product set of Σ_d and Σ_1. This set can be written as $\Sigma_d \cap \Sigma_{K<1}$. Now we focus on the numbers of positive $\tau_{++,+-,--,-+}$ [i.e., $l^{(a)}_{++,+-,--,-+}(\tau)$] that are lower than a certain value of τ. If the sum of the numbers of positive τ_{+-} and τ_{-+} [i.e., $l^{(a)}_{+-}(\tau) + l^{(a)}_{-+}(\tau)$] is equal to the sum of the number of unstable roots at $\tau = 0$ (i.e., 2) and the number of positive τ_{++} and τ_{--} [i.e., $l^{(a)}_{++}(\tau) + l^{(a)}_{--}(\tau)$], then unstable roots at a specific value of τ do not exist. As a result, $g(s, \tau)$ for $(\Delta, K) \in \Sigma_{\Lambda_1}$ is stable for τ belonging to Λ_1, which is the set of τ satisfying this relation.

Third, for region Σ_3, Lemma 4 shows that $g(s, 0)$ has two stable roots. From Lemma 2, we see that, for $\Sigma_{\Lambda_{inf}}$ included in Σ_3, stabilizing or destabilizing points do not exist. Consequently, for $\Sigma_{\Lambda_{inf}}$, the rightmost roots never pass the imaginary axis for any $\tau \in [0, +\infty)$. On the other hand, for Σ_{Λ_3} included in Σ_3, Lemma 2 shows that there exist stabilizing points $i\omega_{-+,+-}$ and destabilizing points $i\omega_{++,--}$. It is straightforward to see that a similar approach to region Σ_{Λ_1} can be used to obtain the intervals for Σ_{Λ_3}.

[1] G. V. Osipov, J. Kurths, and C. Zhou, *Synchronization in Oscillatory Networks* (Springer, Berlin, 2007).
[2] S. Boccaletti, A. N. Pisarchik, C. I. del Genio, and A. Amann, *Synchronization* (Cambridge University, Cambridge, England, 2018).
[3] Y. Yamaguchi and H. Shimizu, Physica D **11**, 212 (1984).
[4] K. Bar-Eli, Physica D **14**, 242 (1985).
[5] R. E. Mirollo and S. H. Strogatz, J. Stat. Phys. **60**, 245 (1990).
[6] D. G. Aronson, G. B. Ermentrout, and N. Kopell, Physica D **41**, 403 (1990).
[7] G. Saxena, A. Prasad, and R. Ramaswamy, Phys. Rep. **521**, 205 (2012).
[8] A. Koseska, E. Volkov, and J. Kurths, Phys. Rep. **531**, 173 (2013).
[9] Y. Sugitani and K. Konishi, NOLTA, IEICE **12**, 612 (2021).
[10] S. R. Huddy and J. D. Skufca, IEEE Trans. Power Electron. **28**, 247 (2013).
[11] T. Biwa, S. Tozuka, and T. Yazaki, Phys. Rev. Appl. **3**, 034006 (2015).
[12] D. V. Ramana Reddy, A. Sen, and G. L. Johnston, Phys. Rev. Lett. **80**, 5109 (1998).
[13] D. V. Ramana Reddy, A. Sen, and G. L. Johnston, Physica D **129**, 15 (1999).
[14] D. V. Ramana Reddy, A. Sen, and G. L. Johnston, Phys. Rev. Lett. **85**, 3381 (2000).
[15] R. Dodla, A. Sen, and G. L. Johnston, Phys. Rev. E **69**, 056217 (2004).
[16] M. P. Mehta and A. Sen, Phys. Lett. A **355**, 202 (2006).
[17] L.B. Le, K. Konishi, and N. Hara, Phys. Rev. E **87**, 042908 (2013).
[18] Y. Sugitani, K. Konishi, L. B. Le, and N. Hara, Chaos **24**, 43105 (2014).
[19] S. R. Huddy and J. Sun, Phys. Rev. E **93**, 052209 (2016).
[20] F. M. Atay, Phys. Rev. Lett. **91**, 094101 (2003).
[21] Y. N. Kyrychko, K. B. Blyuss, and E. Schöll, Philos. Trans. R. Soc. A **371**, 20120466 (2013).
[22] W. Zou and M. Zhan, Phys. Rev. E **80**, 065204(R) (2009).
[23] K. Konishi, H. Kokame, and N. Hara, Phys. Rev. E **81**, 016201 (2010).
[24] K. Konishi, L. B. Le, and N. Hara, Eur. Phys. J. B **85**, 166 (2012).
[25] A. Gjurchinovski, A. Zakharova, and E. Schöll, Phys. Rev. E **89**, 032915 (2014).
[26] Y. Sugitani, K. Konishi, and N. Hara, Phys. Rev. E **92**, 042928 (2015).
[27] W. Zou, D. V. Senthilkumar, R. Nagao, I. Z. Kiss, Y. Tang, A. Koseska, J. Duan, and J. Kurths, Nat. Commun. **6**, 7709 (2015).
[28] K. Okamoto, A. Kijima, Y. Umeno, and H. Shima, Sci. Rep. **6**, 36145 (2016).
[29] K. Manoj, S. A. Pawar, and R. I. Sujith, Sci. Rep. **8**, 11626 (2018).
[30] K. Manoj, S. A. Pawar, S. Dange, S. Mondal, R. I. Sujith, E. Surovyatkina, and J. Kurths, Phys. Rev. E **100**, 062204 (2019).
[31] K. Manoj, S. A. Pawar, and R. I. Sujith, Phys. Rev. E **103**, 022207 (2021).
[32] H. Hyodo and T. Biwa, Phys. Rev. E **98**, 052223 (2018).
[33] N. Thomas, S. Mondal, S. A. Pawar, and R. I. Sujith, Chaos **28**, 033119 (2018).
[34] S. Dange, K. Manoj, S. Banerjee, S. A. Pawar, S. Mondal, and R. I. Sujith, Chaos **29**, 93135 (2019).
[35] H. Hyodo, M. Iwasaki, and T. Biwa, J. Appl. Phys. **128**, 094902 (2020).
[36] K. Moon, Y. Guan, L. K. B. Li, and K. T. Kim, Chaos **30**, 23110 (2020).
[37] A. Raaj, S. Mondal, and V. Jagdish, Int. J. Non-Linear Mech. **129**, 103659 (2021).
[38] R. Xiao, Z. Sun, X. Yang, and W. Xu, Commun. Nonlinear Sci. **69**, 168 (2019).
[39] R. Xiao, Z. Sun, X. Yang, and W. Xu, Nonlinear Dyn. **95**, 2093 (2019).

[40] R. Xiao and Z. Sun, Int. J. Mod. Phys. B **34**, 2050303 (2020).
[41] H. Teki, K. Konishi, and N. Hara, Phys. Rev. E **95**, 062220 (2017).
[42] U. S. Thounaojam and A. Sharma, Chaos, Solitons Fractals **124**, 97 (2019).
[43] A. Sharma, Phys. Lett. A **383**, 1865 (2019).
[44] R. M. Nguimdo, Phys. Rev. E **97**, 032211 (2018).
[45] A. Otto, G. Radons, D. Bachrathy, and G. Orosz, Phys. Rev. E **97**, 012311 (2018).
[46] S. Masamura, T. Iwamoto, Y. Sugitani, K. Konishi, and N. Hara, Nonlinear Dyn. **99**, 3155 (2020).
[47] Y. Okigawa, Y. Sugitani, and K. Konishi, Eur. Phys. J. B **93**, 129 (2020).
[48] N. Zhao and Z. Sun, Int. J. Bifurcation Chaos **30**, 2050094 (2020).
[49] S. R. Huddy, Chaos **30**, 013118 (2020).
[50] J. H. S. Marshall, K. Walton, A. Korytowski, and H. Gorecki, *Time-Delay Systems: Stability and Performance Criteria with Applications* (Horwood, Chichester, 1992).
[51] K. Gu, V. L. Kharitonov, L. Vladimir, and J. Chen, *Stability of Time-Delay Systems* (Springer, Berlin, 2003).
[52] W. Michiels and S.-I. Niculescu, *Stability, Control, and Computation for Time-Delay Systems: An Eigenvalue-Based Approach* (SIAM, Philadelphia, 2014).
[53] R. Sipahi, *Mastering Frequency Domain Techniques for the Stability Analysis of LTI Time Delay Systems* (SIAM, Philadelphia, 2019).
[54] S. Yanchuk, M. Wolfrum, P. Hövel, and E. Schöll, Phys. Rev. E **74**, 026201 (2006).
[55] S. Yanchuk and G. Giacomelli, J. Phys. A **50**, 103001 (2017).
[56] D. Breda, S. Maset, and R. Vermiglio, *Stability of Linear Delay Differential Equations* (Springer, Berlin, 2015).
[57] D. S. Bernstein, *Matrix Mathematics: Theory, Facts, and Formulas*, 2nd ed. (Princeton University, Princeton, NJ, 2009).
[58] B. Thakur, D. Sharma, and A. Sen, Phys. Rev. E **90**, 042904 (2014).
[59] W. Zou, C. Yao, and M. Zhan, Phys. Rev. E **82**, 056203 (2010).
[60] W. Zou, Y. Tang, L. Li, and J. Kurths, Phys. Rev. E **85**, 046206 (2012).
[61] Y. Sugitani and K. Konishi, Phys. Rev. E **96**, 042216 (2017).
[62] W. Zou, M. Zhan, and J. Kurths, Phys. Rev. E **98**, 062209 (2018).